Report

Current Biology

# Uncoordinated sleep replay across hemispheres in the zebra finch

## Graphical abstract

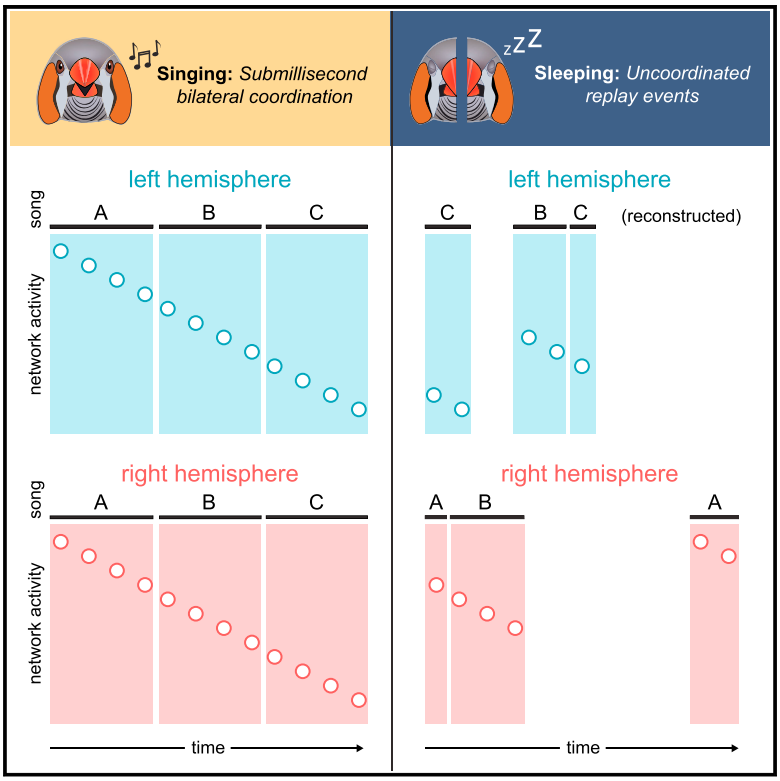


## Highlights

- Monitored population activity of a zebra finch song production nucleus bilaterally
- Left and right coordination within a fraction of a millisecond throughout song
- Largely independent sleep replay across hemispheres despite shared arousal levels

## Authors

Margot Elmaleh, Zetian Yang, Lyn A. Ackert-Smith, Michael A. Long

## Correspondence

mlong@med.nyu.edu

## In brief

By bilaterally monitoring ensemble activity of a key song production nucleus in the zebra finch, Elmaleh et al. show that submillisecond coordination observed during singing is largely absent during sleep, where nonmatching vocal elements are often replayed simultaneously across hemispheres.

Elmaleh et al., 2023, Current Biology *33*, 4704–4712
November 6, 2023 
https://doi.org/10.1016/j.cub.2023.09.005

CellPress

CellPress

Current Biology

Report

# Uncoordinated sleep replay across hemispheres in the zebra finch

Margot Elmaleh,[1,2] Zetian Yang,[1,2] Lyn A. Ackert-Smith,[1,2] and Michael A. Long[1,2,3,*]
[1]NYU Neuroscience Institute and Department of Otolaryngology, New York University Langone Medical Center, New York, NY 10016, USA
[2]Center for Neural Science, New York University, New York, NY 10003, USA
[3]Lead contact
*Correspondence: mlong@med.nyu.edu
https://doi.org/10.1016/j.cub.2023.09.005

## SUMMARY

Bilaterally organized brain regions are often simultaneously active in both humans[1–3] and animal models,[4–9] but the extent to which the temporal progression of internally generated dynamics is coordinated across hemispheres and how this coordination changes with brain state remain poorly understood. To address these issues, we investigated the zebra finch courtship song (duration: 0.5–1.0 s), a highly stereotyped complex behavior[10,11] produced by a set of bilaterally organized nuclei.[12–14] Unilateral lesions to these structures can eliminate or degrade singing,[13,15–17] indicating that both hemispheres are required for song production.[18] Additionally, previous work demonstrated broadly coherent and symmetric bilateral premotor signals during song.[9] To precisely track the temporal evolution of activity in each hemisphere, we recorded bilaterally in the song production pathway. We targeted the robust nucleus of the arcopallium (RA) in the zebra finch, where population activity reflects the moment-to-moment progression of the courtship song during awake vocalizations[19–24] and sleep, where song-related network dynamics reemerge in "replay" events.[24,25] We found that activity in the left and right RA is synchronized within a fraction of a millisecond throughout song. In stark contrast, the two hemispheres displayed largely independent replay activity during sleep, despite shared interhemispheric arousal levels. These findings demonstrate that the degree of bilateral coordination in the zebra finch song system is dynamically modulated by behavioral state.

## RESULTS

### Precise bilateral coordination during courtship song

To characterize the coordination of song activity across hemispheres, we implanted 128-channel silicon probes bilaterally in robust nucleus of the arcopallium (RA) (Figure 1A), the motor cortical output region of the song production circuit. This approach enabled us to record the spiking activity of neural populations in the right (47 ± 14 neurons/bird) and left (46 ± 6 neurons/bird) hemispheres simultaneously in 4 birds (e.g., Figure 1B). During singing, RA neurons in both hemispheres switched from regular tonic firing to high-frequency bursting[19,20] (Figure 1B). We measured the onsets of RA bursts (Figure 1C, 266 ± 117 events/hemisphere; see STAR Methods for inclusion criteria), which have been shown to be temporally locked to vocal production.[19–21] Using this approach, we can leverage RA network activity during song to precisely compare the temporal progression of neural dynamics across the two hemispheres.

We first analyzed the bilateral coordination of motor commands within RA at the level of the syllable (~100–200 ms), a unit of the song that has been shown to be significant both functionally[10,26,27] and developmentally.[28] Using bursting activity across the population of RA neurons, we sought to determine whether trial-to-trial changes in syllable duration[10,11] (e.g., Figures 1B–1D) were equally represented across hemispheres. In our dataset, syllable length varied by 1.3% (interquartile range [IQR]: 0.6%–2.3%, n = 173 trials across 15 syllables). For each syllable trial, the progression of song-related neural activity was measured separately for each hemisphere by comparing the burst times in RA to their mean values across all trials (Figures 1D–1H). We used a linear fit of these RA burst times to estimate network progression. Faster-than-average syllables had negative slopes, and slower-than-average syllables had positive slopes (Figure 1E). We found that these trial slopes were statistically equivalent across hemispheres (Wilcoxon signed-rank, $p = 0.92$, Figures 1G and 1H), indicating that the hemispheres are synchronized at the timescale of syllables (~100 ms) during singing.

To assess hemispheric coordination with subsyllabic precision (i.e., milliseconds), we next calculated the extent to which each individual RA bursting event (see STAR Methods) deviated from a global linear fit for each trial. If the activity of one hemisphere unfolded in a more predictable manner than the other, we would expect comparatively smaller residuals on that hemisphere. However, we find the residuals on the right (median: 0.40 ms, IQR: 0.26–0.66 ms) and the left (median: 0.45 ms, IQR: 0.29–0.76 ms) hemispheres to be statistically equivalent (Wilcoxon rank-sum, $p > 0.05$) in 14 out of 15 syllables across 4 birds (Figure 1I). We further found that regressions based on the activity of the contralateral hemisphere were equally capable of fitting the data as those

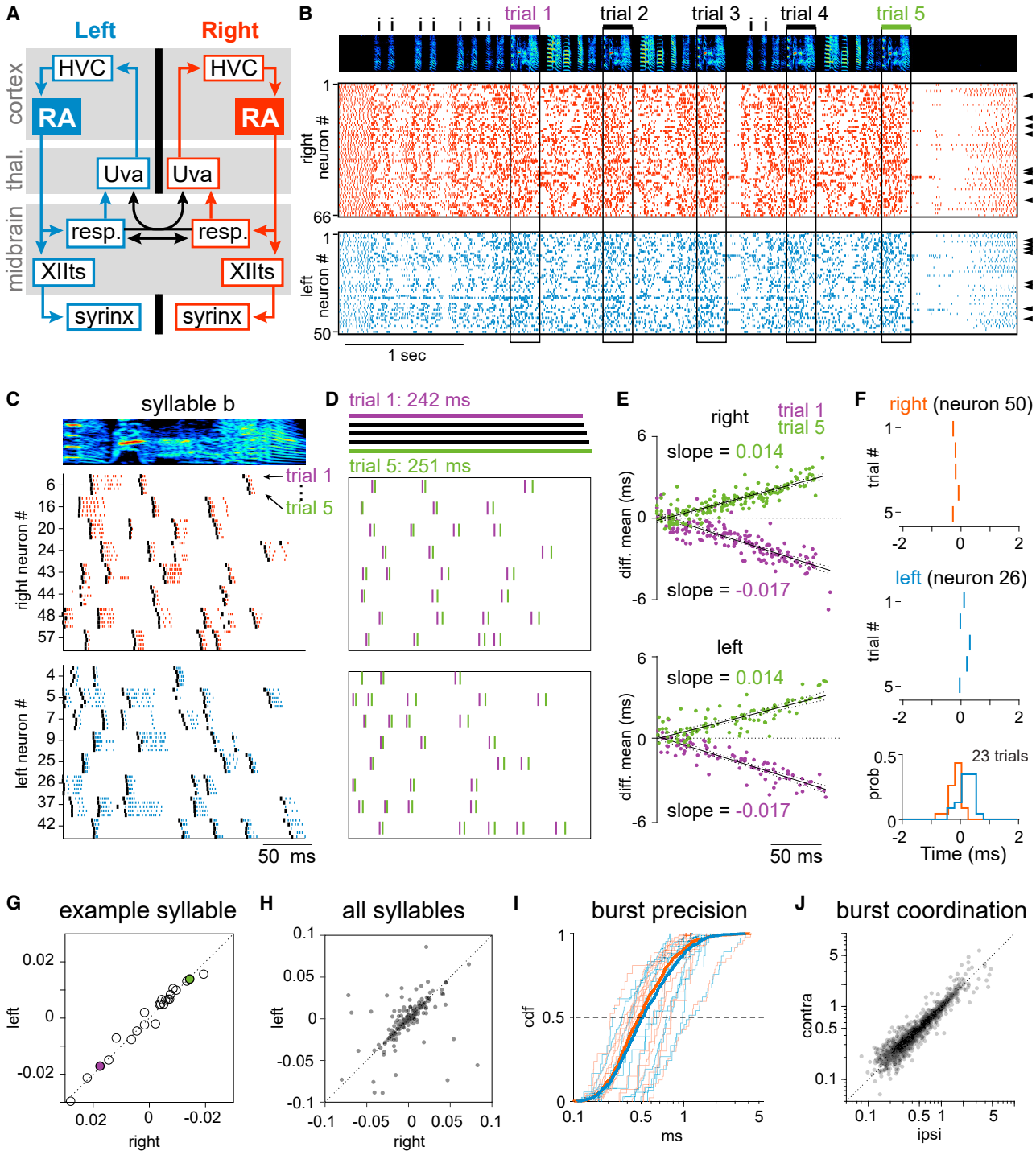


**Figure 1. Bilateral recordings reveal precise interhemispheric coordination during song**

(A) Schematic of the zebra finch bilateral song control system, including HVC (proper name) and the robust nucleus of the arcopallium (RA, the site of neural recordings), the thalamic nucleus uvaeformis (Uva), the midbrain respiratory nuclei ("resp") and the tracheosyringeal region of hypoglossal nucleus (XIIts), and the muscles of the syrinx. Black arrows: anatomical pathways that cross the midline.

(B) Spiking activity of simultaneously recorded RA neurons from the right (red) and left (blue) hemispheres of bird B3 during singing and associated introductory notes (marked with "i") in an adult zebra finch. Syllable "b" occurs 5 times, as noted above the spectrogram. Arrows indicate neurons used in (C).

(C) Spike times of selected RA neurons for five trials of syllable "b" in (B) aligned to syllable onset. Black ticks indicate the first spike from each burst, which defines a burst time.

(D) Song duration and burst timing differ across trials. (Top) Bars indicate the length of each trial of syllable "b" from the song in (B). (Bottom) Tick marks represent the first spike within a burst from (C) for trial 1 (purple) and trial 5 (green).

*(legend continued on next page)*

calculated ipsilaterally (contralateral: 0.42 ms, IQR: 0.28–0.69 ms; ipsilateral: 0.41 ms, IQR: 0.27–0.69 ms; p = 0.18, Wilcoxon sign-rank, n = 1,507 bursts) (Figure 1J), demonstrating submillisecond coordination throughout the song.

## Physiological parameters coordinated across hemispheres during sleep

We next examined whether the high degree of interhemispheric coordination observed during song is an invariant feature of the network or instead is differentially engaged across behavioral states. We shifted our focus to sleep, when the network exhibits song-like activity (i.e., replay events),[25] allowing for a direct comparison of coordination at the level of song-related dynamics across sleep and active singing. We first tested whether the right and left hemispheres were broadly coupled in their global arousal levels and physiological state. Previous work has demonstrated that zebra finches are capable of unihemispheric sleep,[29] specifically during daytime "naps."[30] To examine the prevalence of unihemispheric sleep throughout the night, we used infrared cameras to simultaneously film both eyes (frame rate: 20 Hz)—an indicator of avian sleep[31]—in four head-fixed zebra finches (e.g., Figures 2A and S1A). During these sessions (duration: 8.1 ± 4.5 h), eyes opened and closed symmetrically 98.5% ± 1.2% of the time (Figures 2A, 2B, and S1), and moments of asymmetry were brief (median: 250 ms; IQR: 100–600 ms), indicating that zebra finches were not experiencing unihemispheric sleep in these nighttime observation periods.

To examine the physiological state during sleep in both hemispheres, we monitored brain temperature bilaterally. Previous work in awake zebra finches has demonstrated that rapid changes in brain temperature can also effectively indicate arousal,[32] and temperature is directly related to ongoing neural state in both mammals and birds.[33,34] During sleep, temperature fluctuations ($\Delta T$: $\sim 1^{\circ}C$) significantly covaried across hemispheres (Pearson's corr: $r_{actual} = 0.91 \pm 0.07$, $r_{null} = 0.06 \pm 0.01$; Wilcoxon rank-sum: $p < 0.0001$, n = 3 birds; see STAR Methods; Figures 2C, 2D, and S1B). Furthermore, we observed a negative correlation between temperature and population bursting in RA (Figures 2E, 2F, and S2, $r_{raw} = -0.46 \pm 0.22$, $r_{shuff} = 0.00 \pm 0.27$; Wilcoxon rank-sum: $p < 0.0001$), which is an indicator of replay.[24,25,35,36] This finding suggests that a global signal (i.e., neuromodulatory) may be creating a permissive state for sleep replay that also directly affects brain temperature. Taken together, bilaterally coordinated eye openings and synchronized temperature changes are consistent with a symmetric arousal state across the zebra finch brain during nighttime sleep.

## Degree of bilateral coordination of sleep activity is timescale dependent

To test bilateral coordination of neural activity during sleep, we measured the proportion of time that neurons in each hemisphere spent bursting on the slow timescale over which temperature fluctuates (i.e., ~100 s, Figure 3A). We observed strong correlations of bursting activity between pairs of neurons within ($r_{ipsi} = 0.71 \pm 0.14$) and across ($r_{contra} = 0.62 \pm 0.15$) hemispheres that were significantly greater than expected by chance ($r_{null} = 0.01 \pm 0.03$; Wilcoxon sign-rank: $p < 0.001$, for 7 birds, Figure 3B). These results demonstrate that the general occurrence of bursting—and thus engagement in song replay[24]—is coupled bilaterally in RA during sleep. Although this long timescale coordination is indicative of a bilaterally coherent brain state, sleep replay operates at the temporal resolution relevant for the song system (~milliseconds).[24] We found that the degree of synchronous bilateral bursting (i.e., times when right and left RA were likely both engaged in replay) varied based on the length of our analysis window (Figures 3C, 3D, and S3A). At 1 ms resolution (Figures 3C–3E and S3A), we observed that the amount of time the hemispheres spent bursting together (26.4% ± 8.2%, n = 7 birds) during sleep was categorically different from that observed during song (98.9% ± 1.3%, n = 4 birds). Unilateral bursting could occur in either hemisphere during sleep (e.g., Figure 3F, events i and ii), with a slight preference for the right hemisphere (right: 40.0% ± 6.1%, left: 33.6% ± 8.5%, n = 7 birds, Figures 3G–3J). The relative amount of bilateral and unilateral bursting did not change significantly when comparing 2-h windows taken from the beginning and end of sleep (Wilcoxon sign-rank: $p_{bilateral} = 0.297$, $p_{unilateral} = 0.156$, n = 7). These results indicate that each hemisphere can engage in independent, uncoordinated bursting events on song-related timescales during sleep, suggesting that each hemisphere is capable of separately replaying vocalization-related activity.[24,25]

## Simultaneous sleep replay of different vocal elements across hemispheres

To understand how population bursting in RA relates to vocal behaviors, we used a validated template matching strategy[24] to decode the vocal content of sleep replay events independently for each hemisphere. We expanded upon our prior investigation to include introductory notes and distance calls in addition to song (Figure 4A) to be inclusive of all motor behaviors potentially

(E) Deviation from mean values for all burst times from trials 1 (purple) and 5 (green) of syllable "b" from bird B3 in the right (top) and left (bottom) hemispheres.
(F) Aligned burst onset times for 5 instances of a single burst from neuron 50 (right, top) and neuron 26 (left, middle). Distribution of burst onset times across all trials (n = 23).
(G) Slopes defined by the deviation from mean burst times (E) from each hemisphere for all trials of syllable "b" from example bird B3 (n = 23 trials). Trials 1 and 5 from (D) and (E) are indicated in purple and green, respectively.
(H) Same as in (G) for all syllable renditions (n = 173 trials from 15 syllables) from 4 birds. Not statistically different for 14 out of 15 syllables (Wilcoxon signed-rank: p = 0.92).
(I) Cumulative density functions for the residuals for all burst times on the right (light red) and left (light blue) hemispheres for each syllable (n = 15). Residuals were measured for each trial using a consensus slope calculated with burst times from both hemispheres. Not statistically different (Wilcoxon rank-sum: $p > 0.05$). Thick red and blue lines indicate population data from all 15 syllables.
(J) Mean residuals calculated for each burst time (n = 1,507) using either ipsilateral or contralateral linear fits. Not statistically different (Wilcoxon sign-rank: p = 0.18).

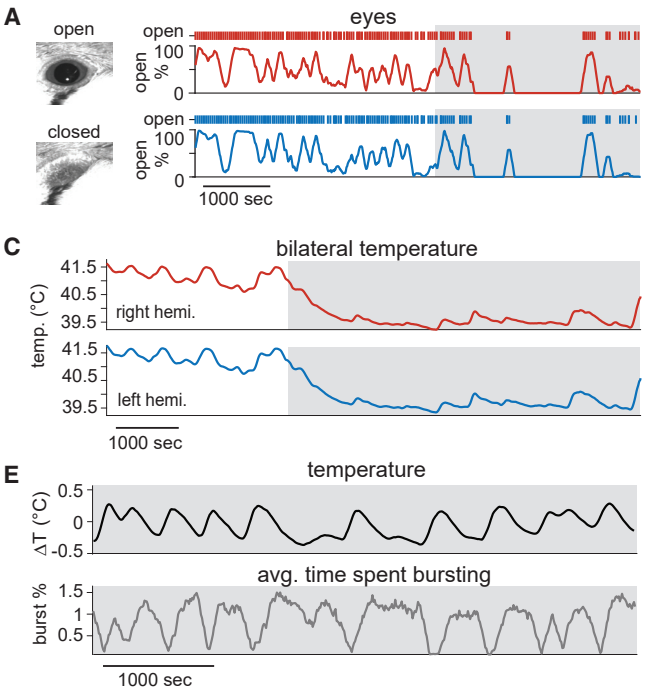


**Figure 2. Interhemispheric symmetry in arousal and physiological state during sleep**

(A) Eye state (example images at left) throughout a portion of the recording period for the left eye (blue) and right eye (red). Ticks at the top indicate frames when an eye was open, and the continuous trace represents the probability of eye opening over a 100-s time window. Shaded region: lights off.

(B) Relationship between the probability of left and right eye opening for bird A413 for the time window shown in (A).

(C) Simultaneous temperature recordings from the right (red) and left (blue) hemispheres of bird BT2. Shaded region: lights off.

(D) Relationship between the temperature values from each hemisphere across the time window shown in (C).

(E) Simultaneous temperature (top) and population bursting percent (bottom, see STAR Methods) during sleep for bird TN1.

(F) Relationship between temperature and neural activity for the time window illustrated in (E). Offset of 90 s was applied to the temperature data, following Figure S2. In (B), (D), and (F), each data point represents a single analysis window (bin width: 100 s, step size: 10 s) for the session depicted in (A), (C), and (E), respectively.

See also Figures S1 and S2.

replayed in RA and thus improve our ability to decode population bursting. We found that no matter the bursting condition (i.e., right only, left only, or coincident bursting), ~75% of replay activity was related to the courtship song. We next turned our attention to periods of coincident sleep bursting to determine whether the two hemispheres are simultaneously replaying different vocal behaviors or if these events exhibit the same high level of bilateral synchrony observed during song. We found that both hemispheres could independently replay different vocal types (e.g., courtship songs, introductory notes, and distance calls; Figures 4B–4D) and did so frequently during sleep (11.2% ± 3.2% of detected replay events were "heterotypic"). To illustrate this effect, we compared the activity of a single replay event (Figure 4B, event iii) to the template activity of two different vocal types (introductory note and syllable "c"; Figure 4C). For this example, replay activity of the left hemisphere matches the introductory note (left), whereas that recorded simultaneously on the right corresponds to song syllable "c" (right). The template matching results highlight the differences in decoded vocal content we observe across hemispheres during periods of coincident bursting (Figure 4D).

When both hemispheres were engaged in replay of the courtship song (i.e., Figure 4E, "homotypic" replay), they only participated in the same syllable 28.9% ± 13.3% of the time. We measured the distance between the two hemispheres with respect to the song template (Figure 4F) throughout the entirety of the sleep period (Figures 4G and S4C) and composed a coordination matrix, which captures the probability density of the coincident vocal content of each hemisphere in relation to our templates for each condition (Figures 4H and 4I). During vocalizations, we find that activity conforms tightly to the unity line (Figures 4H, S4A, and S4B), underscoring the high degree of neural coordination observed. During sleep replay, the disparity in activity between the hemispheres was often significant, diffusely filling the coordination matrix (Figures 4I and S4B) and further reinforcing the notion that the hemispheres can act independently when simultaneously engaged in replay. We find that the median estimated song distance between the two hemispheres during sleep was 53.6 ms (IQR: 8.6–183 ms, Figures 4F, 4G, and 4I–4K). This is in stark contrast to what is observed during song (Figures 1, 4H, and S4A), where the hemispheres are highly coordinated (Figures 4H–4K, S4A, and S4C, median estimated temporal distance: 1.9 ms, IQR: 0–3.8 ms, Wilcoxon rank-sum: $p < 0.0001$). Therefore, the strict coordination between hemispheres exhibited during vocal production is absent during the sleep replay of those same vocalizations.

## DISCUSSION

In this study, we leverage the relationship between behavior and neural activity in the zebra finch song system to investigate the temporal coordination of neural processing across hemispheres. We find that activity within the song production nucleus RA unfolds bilaterally with submillisecond precision during singing, whereas these same network dynamics can reemerge independently during sleep. These brain state related changes in hemispheric coordination were observed in forebrain (cortical) areas of the zebra finch song circuit, which are not directly connected across hemispheres (Figure 1A), unlike in mammalian systems where reciprocal projections are mediated by the corpus callosum[37] or other interhemispheric pathways.[38,39] This strict unilateral organization is maintained down to the periphery, establishing segregated descending motor control pathways.[12] Previous electromyogram (EMG) recordings have revealed that activity in vocal tract musculature is precisely coordinated during song[40–42] and poorly coordinated during sleep.[43] Here, we

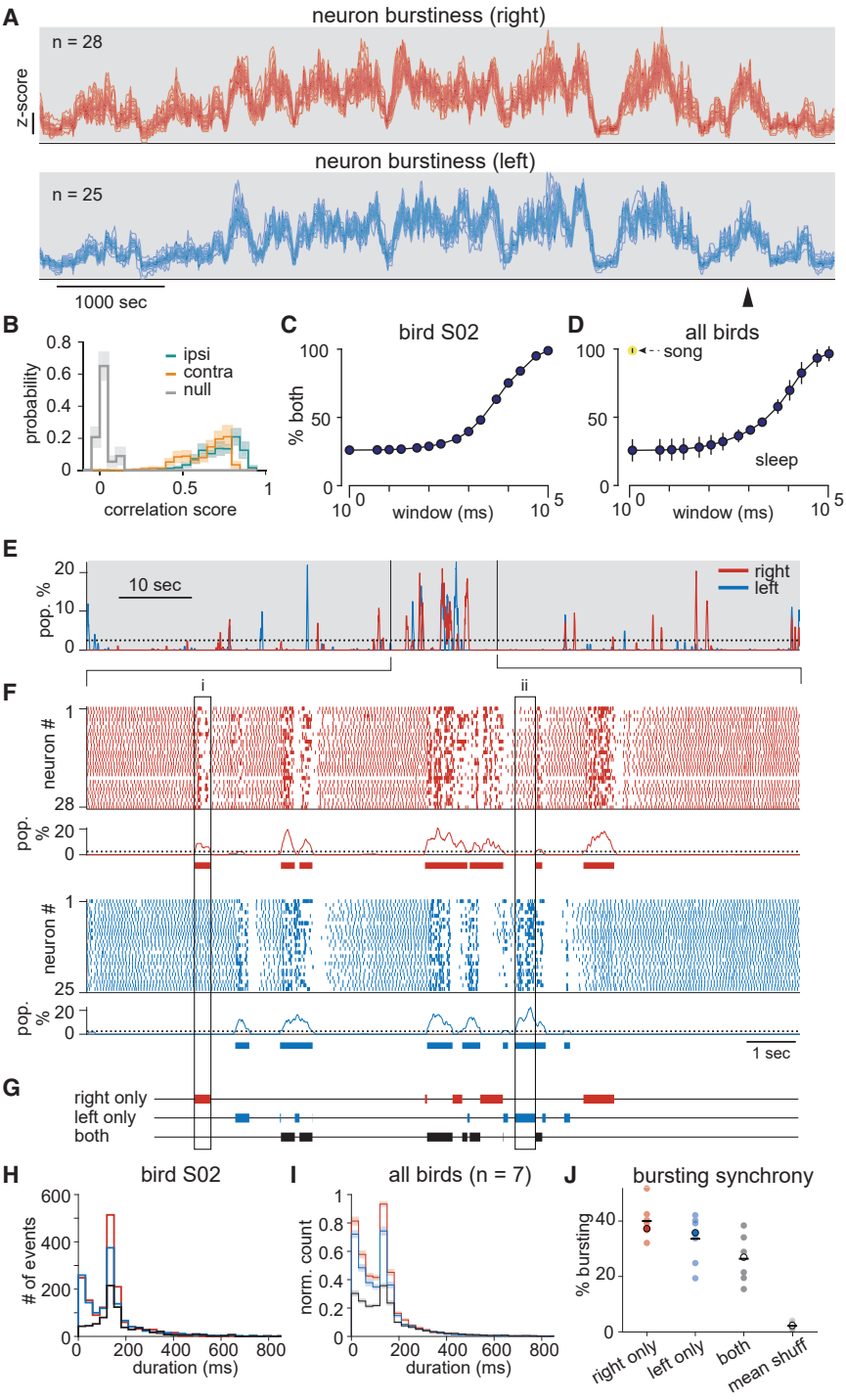


**Figure 3. Degree of bilateral coordination in sleep activity across timescales**

(A) Normalized percentage of time spent bursting during sleep for individual RA neurons recorded from the right (red) and left (blue) hemispheres from bird S02.

(B) Correlation scores (mean ± SEM) for ipsilateral (teal), contralateral (orange), and shuffled (gray) pairwise comparisons of burstiness between neurons (see STAR Methods). The correlation scores between contralateral pairs were statistically different than those expected by chance (Wilcoxon sign-rank test: p = 0.001, n = 7 birds).

(C and D) Bilateral population burst coordination changes with the size of analysis window. Percent of total time that both hemispheres burst together during sleep for bird S02 (C). Population data (mean ± SD) for seven birds during sleep (dark blue data points) across all windows and for four birds during song (window size: 1 ms) indicated by yellow data point (D).

(E) Percentage of neurons from the recorded population bursting moment-to-moment (bin size: 5 ms) on the right (red) and left (blue) hemispheres for bird S02 during sleep.

(F and G) An expanded epoch from (E), indicated by vertical lines, showing spiking activity for all recorded neurons from the right (red) and left (blue) hemispheres. Population burst percentage is given below. Horizontal bars in (G) represent times in which this value exceeds a predetermined threshold (see STAR Methods) indicated by dashed lines in (F), for right-only bursting (red), left-only bursting (blue), or simultaneous left/right bursting (black). Boxes highlight examples in which only a single hemisphere is bursting (i, right only; ii, left only).

(H and I) Distribution of burst event durations (red, right only; blue, left only; and black, both) for bird S02 (H) and for all 7 birds (I). Shaded regions in (I) represent SEM.

(J) Percentage of time spent bursting independently and together compared with a shuffled distribution (mean reported for each bird, see STAR Methods). Dots represent values from individual birds (n = 7). Outlined symbols indicate example bird S02 shown above. Horizontal lines are the mean values across all birds.

See also Figure S3.

extend these observations by decoding the behavioral content of neural activity both during active singing and sleep and by contextualizing these observations with global measures of synchronized arousal.

The precise bilateral synchrony we observe during singing suggests that coordination stems from a dedicated network mechanism, perhaps through common external input.[9,44,45] In the zebra finch, the motor thalamic nucleus uvaeformis (Uva) relays information about song sequence timing from bilateral respiratory centers to the song forebrain nuclei in each hemisphere and is therefore well-positioned to provide such a coordinating signal (Figure 1A).[9,17,44–47] Recent work showed thalamic input from Uva selectively activates a subset of premotor neurons in HVC (proper name) that fire at syllable onsets,[27] and the coordinated initiation of these "starter neurons" on both hemispheres may enable the submillisecond precision observed while singing.[9,17,48,49] Our results suggest that the nature of this thalamic drive may be fundamentally altered during sleep, consistent with previous findings[24] in which sleep has been associated with a decrease in thalamic efficacy and cortical receptivity to thalamic inputs[50–52] due

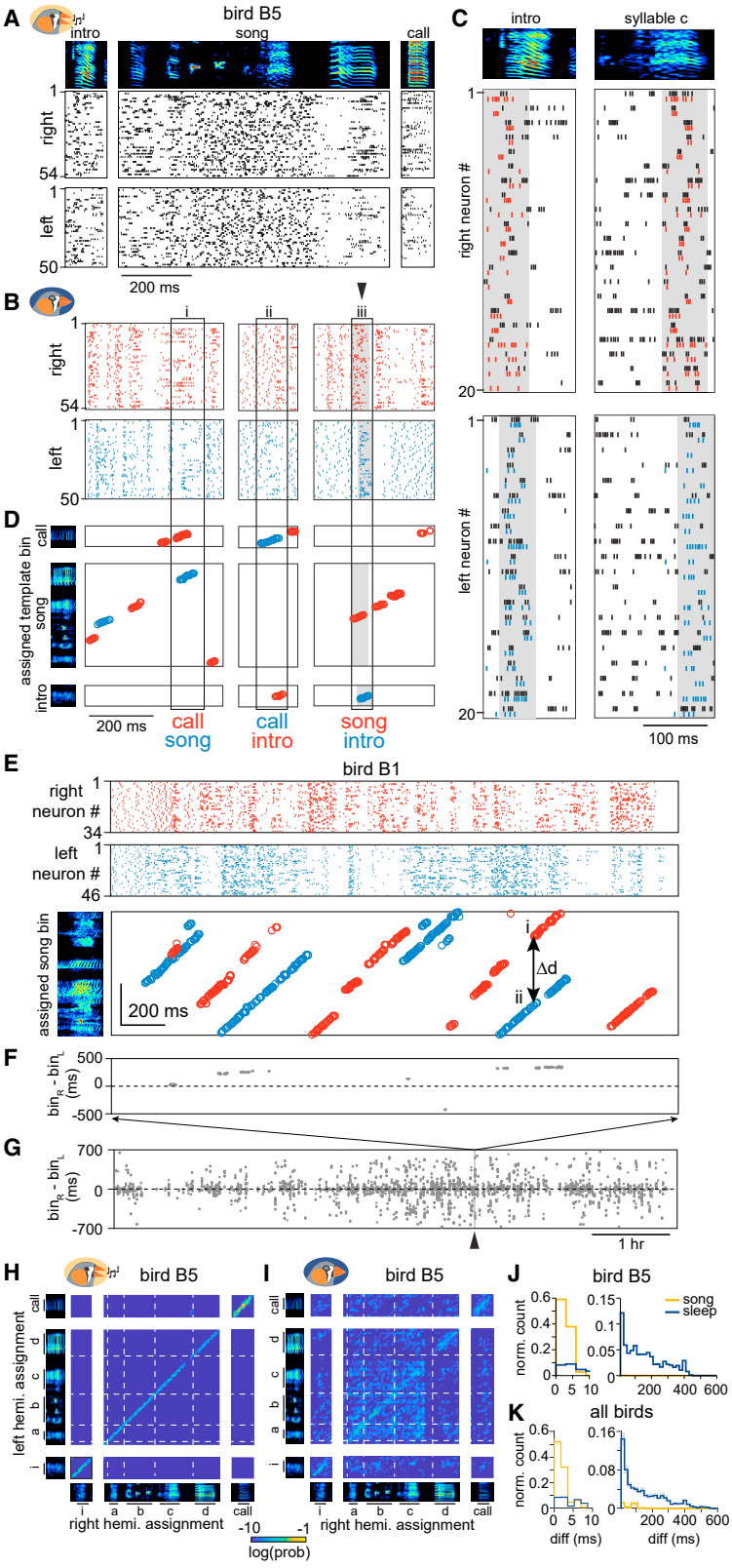


**Figure 4. Reconstructed sleep replay is poorly synchronized across hemispheres**

(A) Spiking activity of simultaneously recorded neurons on the right and left hemispheres from bird B5 during an introductory note, a song motif, and a call.

(B) Three examples (i–iii) of coincident left/right bursting activity from bird B5 during sleep (same neurons as in A). Red, right; blue, left.

(C) A closer view of sleep activity, indicated by arrow in (B), in which activity of 20 example neurons from each hemisphere (top, red, right hemisphere; bottom, blue, left hemisphere) is interleaved with the vocalization activity of those same 20 neurons during either an introductory note (left) or syllable "c" (right). Shaded portion indicates when neurons were bursting in each hemisphere during sleep (Figure B, epoch iii).

(D) Decoding sleep activity using network activity recorded during vocal production (A). Each panel shows the time in the vocalization template (i.e., bin assignment) that contains neural activity most similar to that occurring during sleep. Bin assignments are marked by circles (red, right; blue, left). Examples highlighted by black boxes (i–iii) show moments in which burst patterns exhibit heterotypic replay, defined as the simultaneous appearance of song and nonsong vocalizations (i.e., call or introductory note).

(E) Simultaneous homotypic replay of singing activity across hemispheres for bird B1. Spiking activity for all neurons recorded is shown at the top, with decoded bin assignments below.

(F and G) The song distance between decoded sleep replay across hemispheres for the example provided above (F) and for the entire duration of the sleep recording period (7.4 h) (G).

(H and I) Coordination matrix illustrating the probability density distribution of the relationship between the assigned template location for activity during vocalizations (H) and sleep (I) across hemispheres for bird B5 for introductory notes, songs, and calls. Matrix bin size: 10 ms.

(J and K) The temporal difference between bin assignments in the left and right hemispheres during song (yellow) and sleep replay of the song (dark blue) for bird B5 (J) and for all 4 birds (K) (mean ± SEM). Statistically different (Wilcoxon rank-sum: $p < 0.0001$).

See also Figure S4.

to changes in neuromodulatory tone.[53,54] Additionally, the patterned breathing observed during singing[55,56] is absent during sleep,[43] suggesting that Uva may no longer have access to bilateral information about the ongoing vocal content of replay events via respiratory nuclei to coordinate the hemispheres at night. The possibility exists that these missing respiratory-related inputs from brainstem centers may contain critical timing cues for allowing Uva to properly engage cortical targets during song.

Functional uncoupling of bilateral song nuclei during sleep (i.e., uncoordinated replay) does not appear to have a clear deleterious effect on singing in the adult zebra finch, as adult song performance remains stable before and after sleep.[22,57] This indicates that if sleep replay is playing an important role in adult song maintenance, the mechanisms are likely unilateral and are unlikely to require nighttime coordination. Whether a lack of replay coordination leads to the observed degradation of singing after sleep in juvenile birds[57] remains to be investigated. The possibility exists that unihemispheric sleep may instead provide several advantages in the zebra finch song circuit, including maintaining local network precision[22,53] and facilitating learning.[35,57,58] Specialized inhibitory circuitry has been characterized[59] to facilitate active uncoupling of bilateral structures, which may play an important role in mediating motor control[60] and sensory processing.[61] Recent work exploring the neural circuits mediating hemispheric competition during sleep[62] provides the foundation for future studies to explore the mechanisms by which the left and right hemispheres are dynamically coordinated with brain state across species. Our results suggest that changes in behaviorally relevant hemispheric coupling could be a general mechanism across taxa to adapt neural function to different contexts.

## STAR★METHODS

Detailed methods are provided in the online version of this paper and include the following:

- KEY RESOURCES TABLE
- RESOURCE AVAILABILITY
  - Lead contact
  - Materials availability
  - Data and code availability
- EXPERIMENTAL MODEL AND SUBJECT DETAILS
- METHOD DETAILS
  - Surgical procedures
  - Extracellular Recordings
  - Quantification and statistical analysis

## SUPPLEMENTAL INFORMATION

Supplemental information can be found online at https://doi.org/10.1016/j.cub.2023.09.005.

## ACKNOWLEDGMENTS

This research was supported by the NIH F31 NS116933 (M.E.), the NIH R01 NS075044 (M.A.L.), and the Simons Global Brain (M.A.L.). We thank Lorenz Fenk, Daniel Bendor, Marc Schmidt, Felix Moll, Ipshita Zutshi, and members of the Long laboratory for comments on earlier versions of this manuscript. Abby Paulson provided technical assistance.

## AUTHOR CONTRIBUTIONS

M.E. and M.A.L. conceived the study and designed the experiments. M.E. and Z.Y. conducted the research. M.E., Z.Y., L.A.A.-S., and M.A.L. performed data analysis. M.E. and M.A.L. created the figures. M.E. wrote the initial draft of the manuscript. M.E., Z.Y., L.A.A.-S., and M.A.L. edited and reviewed the final manuscript. M.E. and M.A.L. acquired funding. M.A.L. supervised the project.

## DECLARATION OF INTERESTS

The authors declare no competing interests.

Received: April 5, 2023
Revised: June 28, 2023
Accepted: September 1, 2023
Published: September 26, 2023

## REFERENCES

1. Biswal, B., Yetkin, F.Z., Haughton, V.M., and Hyde, J.S. (1995). Functional connectivity in the motor cortex of resting human brain using echo-planar MRI. Magn. Reson. Med. *34*, 537–541.
2. Iwama, S., Yanagisawa, T., Hirose, R., and Ushiba, J. (2022). Beta rhythmicity in human motor cortex reflects neural population coupling that modulates subsequent finger coordination stability. Commun. Biol. *5*, 1375.
3. Riecker, A., Mathiak, K., Wildgruber, D., Erb, M., Hertrich, I., Grodd, W., and Ackermann, H. (2005). fMRI reveals two distinct cerebral networks subserving speech motor control. Neurology *64*, 700–706.
4. Vanni, M.P., and Murphy, T.H. (2014). Mesoscale transcranial spontaneous activity mapping in GCaMP3 transgenic mice reveals extensive reciprocal connections between areas of somatomotor cortex. J. Neurosci. *34*, 15931–15946.
5. Guan, H., Middleton, S.J., Inoue, T., and McHugh, T.J. (2021). Lateralization of CA1 assemblies in the absence of CA3 input. Nat. Commun. *12*, 6114.
6. Carr, M.F., Karlsson, M.P., and Frank, L.M. (2012). Transient slow gamma synchrony underlies hippocampal memory replay. Neuron *75*, 700–713.
7. Chen, G., Kang, B., Lindsey, J., Druckmann, S., and Li, N. (2021). Modularity and robustness of frontal cortical networks. Cell *184*, 3717–3730.e24.
8. Li, N., Daie, K., Svoboda, K., and Druckmann, S. (2016). Robust neuronal dynamics in premotor cortex during motor planning. Nature *532*, 459–464.
9. Schmidt, M.F. (2003). Pattern of interhemispheric synchronization in HVc during singing correlates with key transitions in the song pattern. J. Neurophysiol. *90*, 3931–3949.
10. Glaze, C.M., and Troyer, T.W. (2006). Temporal structure in zebra finch song: implications for motor coding. J. Neurosci. *26*, 991–1005.
11. Lombardino, A.J., and Nottebohm, F. (2000). Age at deafening affects the stability of learned song in adult male zebra finches. J. Neurosci. *20*, 5054–5064.
12. Wild, J.M., Williams, M.N., and Suthers, R.A. (2000). Neural pathways for bilateral vocal control in songbirds. J. Comp. Neurol. *423*, 413–426.
13. Nottebohm, F., Stokes, T.M., and Leonard, C.M. (1976). Central control of song in the canary, Serinus canarius. J. Comp. Neurol. *165*, 457–486.
14. Nottebohm, F., Kelley, D.B., and Paton, J.A. (1982). Connections of vocal control nuclei in the canary telencephalon. J. Comp. Neurol. *207*, 344–357.
15. Williams, H., and Vicario, D.S. (1993). Temporal patterning of song production: participation of nucleus uvaeformis of the thalamus. J. Neurobiol. *24*, 903–912.

16. Coleman, M.J., and Vu, E.T. (2005). Recovery of impaired songs following unilateral but not bilateral lesions of nucleus uvaeformis of adult zebra finches. J. Neurobiol. *63*, 70–89.

17. Ashmore, R.C., Bourjaily, M., and Schmidt, M.F. (2008). Hemispheric coordination is necessary for song production in adult birds: implications for a dual role for forebrain nuclei in vocal motor control. J. Neurophysiol. *99*, 373–385.

18. Vu, E.T., Schmidt, M.F., and Mazurek, M.E. (1998). Interhemispheric coordination of premotor neural activity during singing in adult zebra finches. J. Neurosci. *18*, 9088–9098.

19. Yu, A.C., and Margoliash, D. (1996). Temporal hierarchical control of singing in birds. Science *273*, 1871–1875.

20. Leonardo, A., and Fee, M.S. (2005). Ensemble coding of vocal control in birdsong. J. Neurosci. *25*, 652–661.

21. Chi, Z., and Margoliash, D. (2001). Temporal precision and temporal drift in brain and behavior of zebra finch song. Neuron *32*, 899–910.

22. Rauske, P.L., Chi, Z., Dave, A.S., and Margoliash, D. (2010). Neuronal stability and drift across periods of sleep: premotor activity patterns in a vocal control nucleus of adult zebra finches. J. Neurosci. *30*, 2783–2794.

23. Egger, R., Tupikov, Y., Elmaleh, M., Katlowitz, K.A., Benezra, S.E., Picardo, M.A., Moll, F., Kornfeld, J., Jin, D.Z., and Long, M.A. (2020). Local axonal conduction shapes the spatiotemporal properties of neural sequences. Cell *183*, 537–548.e12.

24. Elmaleh, M., Kranz, D., Asensio, A.C., Moll, F.W., and Long, M.A. (2021). Sleep replay reveals premotor circuit structure for a skilled behavior. Neuron *109*, 3851–3861.e4.

25. Dave, A.S., and Margoliash, D. (2000). Song replay during sleep and computational rules for sensorimotor vocal learning. Science *290*, 812–816.

26. Cynx, J. (1990). Experimental determination of a unit of song production in the zebra finch (Taeniopygia guttata). J. Comp. Psychol. *104*, 3–10.

27. Moll, F.W., Kranz, D., Corredera Asensio, A., Elmaleh, M., Ackert-Smith, L.A., and Long, M.A. (2023). Thalamus drives vocal onsets in the zebra finch courtship song. Nature *616*, 132–136.

28. Lipkind, D., Marcus, G.F., Bemis, D.K., Sasahara, K., Jacoby, N., Takahasi, M., Suzuki, K., Feher, O., Ravbar, P., Okanoya, K., et al. (2013). Stepwise acquisition of vocal combinatorial capacity in songbirds and human infants. Nature *498*, 104–108.

29. Rattenborg, N.C., Amlaner, C.J., and Lima, S.L. (2000). Behavioral, neurophysiological and evolutionary perspectives on unihemispheric sleep. Neurosci. Biobehav. Rev. *24*, 817–842.

30. Low, P.S., Shank, S.S., Sejnowski, T.J., and Margoliash, D. (2008). Mammalian-like features of sleep structure in zebra finches. Proc. Natl. Acad. Sci. USA *105*, 9081–9086.

31. Amlaner, C. (1988). Asynchronous eye-closure and unihemispheric quiet sleep of birds. In Sleep '86: Proceedings of the Eight European Congress on Sleep Research, Szeged (Gustav Fischer Verlag).

32. Aronov, D., and Fee, M.S. (2012). Natural changes in brain temperature underlie variations in song tempo during a mating behavior. PLoS One *7*, e47856.

33. Kawamura, H., and Sawyer, C.H. (1965). Elevation in brain temperature during paradoxical sleep. Science *150*, 912–913.

34. Hayward, J.N., and Baker, M.A. (1969). A comparative study of the role of the cerebral arterial blood in the regulation of brain temperature in five mammals. Brain Res. *16*, 417–440.

35. Shank, S.S., and Margoliash, D. (2009). Sleep and sensorimotor integration during early vocal learning in a songbird. Nature *458*, 73–77.

36. Shea, S.D., and Margoliash, D. (2010). Behavioral state-dependent reconfiguration of song-related network activity and cholinergic systems. J. Chem. Neuroanat. *39*, 132–140.

37. Roland, J.L., Snyder, A.Z., Hacker, C.D., Mitra, A., Shimony, J.S., Limbrick, D.D., Raichle, M.E., Smyth, M.D., and Leuthardt, E.C. (2017). On the role of the corpus callosum in interhemispheric functional connectivity in humans. Proc. Natl. Acad. Sci. USA *114*, 13278–13283.

38. Paterson, A.K., and Bottjer, S.W. (2017). Cortical inter-hemispheric circuits for multimodal vocal learning in songbirds. J. Comp. Neurol. *525*, 3312–3340.

39. Suárez, R., Gobius, I., and Richards, L.J. (2014). Evolution and development of interhemispheric connections in the vertebrate forebrain. Front. Hum. Neurosci. *8*, 497.

40. Nottebohm, F. (1971). Neural lateralization of vocal control in a passerine bird. I. Song. J. Exp. Zool. *177*, 229–261.

41. Goller, F., and Suthers, R.A. (1996). Role of syringeal muscles in gating airflow and sound production in singing brown thrashers. J. Neurophysiol. *75*, 867–876.

42. Goller, F., and Cooper, B.G. (2004). Peripheral motor dynamics of song production in the zebra finch. Ann. N. Y. Acad. Sci. *1016*, 130–152.

43. Young, B.K., Mindlin, G.B., Arneodo, E., and Goller, F. (2017). Adult zebra finches rehearse highly variable song patterns during sleep. PeerJ *5*, e4052.

44. Schmidt, M.F. (2008). Using both sides of your brain: the case for rapid interhemispheric switching. PLoS Biol. *6*, e269.

45. Striedter, G.F., and Vu, E.T. (1998). Bilateral feedback projections to the forebrain in the premotor network for singing in zebra finches. J. Neurobiol. *34*, 27–40.

46. Ashmore, R.C., Renk, J.A., and Schmidt, M.F. (2008). Bottom-up activation of the vocal motor forebrain by the respiratory brainstem. J. Neurosci. *28*, 2613–2623.

47. Luma, A.Y., Perez, C.I., Pimentel-Farfan, A.K., Báez-Cordero, A.S., González-Pereyra, P., Ortega-Romero, D.I., Martinez-Montalvo, M.G., Peña-Rangel, T.M., and Rueda-Orozco, P.E. (2022). The central medial thalamic nucleus facilitates bilateral movement execution in rats. Neuroscience *499*, 118–129.

48. Long, M.A., Jin, D.Z., and Fee, M.S. (2010). Support for a synaptic chain model of neuronal sequence generation. Nature *468*, 394–399.

49. Logiaco, L., and Abbott, L.F. (2021). Thalamic control of cortical dynamics in a model of flexible motor sequencing. Cell Rep. *35*, 109090.

50. Llinás, R.R., and Paré, D. (1991). Of dreaming and wakefulness. Neuroscience *44*, 521–535.

51. Pape, H.C., and McCormick, D.A. (1989). Noradrenaline and serotonin selectively modulate thalamic burst firing by enhancing a hyperpolarization-activated cation current. Nature *340*, 715–718.

52. Logothetis, N.K., Eschenko, O., Murayama, Y., Augath, M., Steudel, T., Evrard, H.C., Besserve, M., and Oeltermann, A. (2012). Hippocampal–cortical interaction during periods of subcortical silence. Nature *491*, 547–553.

53. Dave, A.S., Yu, A.C., and Margoliash, D. (1998). Behavioral state modulation of auditory activity in a vocal motor system. Science *282*, 2250–2254.

54. Cardin, J.A., and Schmidt, M.F. (2004). Noradrenergic inputs mediate state dependence of auditory responses in the avian song system. J. Neurosci. *24*, 7745–7753.

55. Franz, M., and Goller, F. (2002). Respiratory units of motor production and song imitation in the zebra finch. J. Neurobiol. *51*, 129–141.

56. Veit, L., Aronov, D., and Fee, M.S. (2011). Learning to breathe and sing: development of respiratory-vocal coordination in young songbirds. J. Neurophysiol. *106*, 1747–1765.

57. Derégnaucourt, S., Mitra, P.P., Fehér, O., Pytte, C., and Tchernichovski, O. (2005). How sleep affects the developmental learning of bird song. Nature *433*, 710–716.

58. Tchernichovski, O., Mitra, P.P., Lints, T., and Nottebohm, F. (2001). Dynamics of the vocal imitation process: how a zebra finch learns its song. Science *291*, 2564–2569.

59. Palmer, L.M., Schulz, J.M., Murphy, S.C., Ledergerber, D., Murayama, M., and Larkum, M.E. (2012). The cellular basis of $GABA_B$-mediated interhemispheric inhibition. Science *335*, 989–993.

60. Geffen, G.M., Jones, D.L., and Geffen, L.B. (1994). Interhemispheric control of manual motor activity. Behav. Brain Res. *64*, 131–140.

61. Forss, N., Hietanen, M., Salonen, O., and Hari, R. (1999). Modified activation of somatosensory cortical network in patients with right-hemisphere stroke. Brain *122*, 1889–1899.

62. Fenk, L.A., Riquelme, J.L., and Laurent, G. (2023). Interhemispheric competition during sleep. Nature *616*, 312–318.

63. Pachitariu, M., Steinmetz, N., Kadir, S., Carandini, M., and Harris, K.D. (2016). Kilosort: realtime spike-sorting for extracellular electrophysiology with hundreds of channels. Preprint at bioRxiv.

64. Yang, L., Lee, K., Villagracia, J., and Masmanidis, S.C. (2020). Open source silicon microprobes for high throughput neural recording. J. Neural Eng. *17*, 016036.

65. Picardo, M.A., Merel, J., Katlowitz, K.A., Vallentin, D., Okobi, D.E., Benezra, S.E., Clary, R.C., Pnevmatikakis, E.A., Paninski, L., and Long, M.A. (2016). Population-level representation of a temporal sequence underlying song production in the zebra finch. Neuron *90*, 866–876.

66. Rossant, C., Kadir, S.N., Goodman, D.F.M., Schulman, J., Hunter, M.L.D., Saleem, A.B., Grosmark, A., Belluscio, M., Denfield, G.H., Ecker, A.S., et al. (2016). Spike sorting for large, dense electrode arrays. Nat. Neurosci. *19*, 634–641.

## STAR★METHODS

### KEY RESOURCES TABLE

| REAGENT or RESOURCE | SOURCE | IDENTIFIER |
|---|---|---|
| Chemicals, peptides, and recombinant proteins | | |
| DiI | Thermo Fisher Scientific | V22885 |
| Deposited data | | |
| Neural and accompanying data | This paper | Open Science Framework: https://osf.io/8wfz6/ https://doi.org/10.17605/OSF.IO/8WFZ6 |
| Experimental models: Organisms/strains | | |
| Zebra finch (Taeniopygia guttata) | Magnolia Bird Farm, Anaheim, CA | N/A |
| Software and algorithms | | |
| MATLAB | MathWorks | https://www.mathworks.com/products/matlab.html |
| Camera acquisition software | FLIR | FlyCapture |
| KiloSort spike sorting software | Pachitariu et al.[63] | https://github.com/cortex-lab/KiloSort |
| Vocal-content decoder (Template-matching tool) | This paper | Open Science Framework: https://osf.io/8wfz6/ https://doi.org/10.17605/OSF.IO/8WFZ6 |
| Other | | |
| High-density silicon probe | Diagnostic Biochips | 128-5 integrated |
| High-density silicon probe | S. Masmanidis, UCLA | 64-H |
| SLA printer | Formlabs | Form2 |
| SLA resin | Formlabs | Clear V4 |
| Camera | FLIR | Grasshopper3 |
| Thermocouple | Omega | 5SRTC-TT-K-40-36-ROHS |
| Thermocouple amplifier | Omega | DP8PT-006 |
| Assisted Fiber-optic & Electric Rotary Joint | Doric Lenses | AHRJ-OE_FC_AD_12_HARW |
| Omnetics cable adaptor | Doric Lenses | ADAPTER_HO12 |
| Acquisition board | Intan Technologies | RHD Recording Controller (512 channels) |
| Omnidirectional microphone | Audio-Technica | AT803 |
| Audio amplifier | Presonus | Studio Channel |

### RESOURCE AVAILABILITY

#### Lead contact

Further information and requests for resources and reagents should be directed to and will be fulfilled by the Lead Contact, Michael Long (mlong@med.nyu.edu).

#### Materials availability

This study did not generate new unique reagents.

#### Data and code availability

The central data sets and code generated during this study have been deposited on the Open Science Framework and are publicly available as of the date of publication. DOIs are listed in the key resources table. Any additional information required to reanalyze the data reported in this paper is available from the lead contact upon request.

### EXPERIMENTAL MODEL AND SUBJECT DETAILS

We used adult (> 90 days posthatch) male zebra finches (*Taeniopygia guttata*) that were obtained from an outside breeder and maintained in a temperature- and humidity-controlled environment with a 12/12 hr light/dark schedule. All animal maintenance and experimental procedures were performed according to the guidelines established by the Institutional Animal Care and Use Committee at the New York University Langone Medical Center.

## METHOD DETAILS

### Surgical procedures

All surgical procedures were performed under isoflurane anesthesia (1%–3% in oxygen) following established guidelines. The animals used in acute recordings were implanted with a headplate for secure head-fixation prior to the experiment day. Details pertaining to the use of high-density silicon probes for chronic recordings have been described elsewhere.[23] Here, silicon probes were lowered sequentially into the robust nucleus of the archipallium (RA) of each hemisphere, using the bifurcation of the sagittal sinus as the stereotaxic origin (craniotomy: 2.35 mm lateral and 0.1 mm posterior). The ground wire was inserted between the skull and the dura above the cerebellum along the midline for the left probe and lateral to the craniotomy for the right probe. Silicon elastomer (Kwik-Cast, WPI) was applied to the craniotomy once the target region was successfully identified on > 50% of channels (depth: ~2.5-3 mm) using the Intan Recording system (Intan USB evaluation board or RHD Recording Controller). By tracking the electrical activity across our electrodes, we could optimize the placement to maximize the number of channels within RA. For chronic recordings, our electrodes spanned 450 μm anterior-posterior and 300 μm dorsal-ventral, which ensured that we could record simultaneously from a significant portion of RA, which is ~ 750 μm in diameter.

### Extracellular Recordings

Chronic recordings were performed using two integrated 128-channel high-density silicon probes (Diagnostic Biochips, 128-5) in each animal. Prior to surgery, a stainless-steel ground wire (diameter: 0.001", AM systems) was soldered to the reference of the headstage, which was held in place by a custom-made 3D printed enclosure (Formlabs). Within the hour following surgery, we began continuously recording neural activity bilaterally (Intan RHD Recording Controller) and all vocalizations using an omnidirectional microphone (Audio-Technica) and an analog preamplifier (Presonus). Free movement was enabled by an electrically assisted commutator (Doric Lenses). Female zebra finches were placed in an adjacent cage to elicit song.

For the acute bilateral recordings, a 64-channel silicon probe (S. Masmanidis, UCLA; 64-H)[64] was lowered into each hemisphere as described above. Both eyes were monitored using CMOS cameras (FLIR, Grasshopper3, Frame rate: 20 Hz). Individual frames were triggered by an external source (Master 9) and acquired using FlyCapture software. The trigger signal was simultaneously acquired through the Intan Recording Controller to ensure common time stamps with neural data. In one instance, an expertly trained head-fixed singer[65] was used (bird A413). Once the probes were in place, an automated curtain revealed a female in front of the head-fixed bird. After successful song, the female was removed, and the lights were turned off. The three other acute bilateral recordings were performed using birds habituated to sleeping in a foam restraint while head-fixed.

The simultaneous temperature and neural recordings were performed in head-fixed animals with a 128-channel silicon probe (Diagnostic Biochips, 128-5) in RA of the right hemisphere and a thermocouple (Omega: 5SRTC-TT-K-40-36-ROHS) lowered ~ 2 mm into the left hemisphere through a craniotomy with the same coordinates as that on the right. The temperature signal was amplified (Omega: DP8PT-006) and acquired using the Intan Recording Controller along with the neural signal. Bilateral temperature recordings were performed across lighting conditions (i.e., with > 1 hr each of lights on and off).

#### *Recording neural activity during vocalizations and sleep*

Automated spike detection and sorting was carried out using Kilosort software[63] and manual post-processing was performed using Phy[66] as described previously.[23] Custom MATLAB software was used to analyze audio recordings and to align single unit data to behavior. To identify burst times across song renditions, we established a canonical bursting pattern for each neuron using song-aligned spiking activity. We defined bursts as events with an inter-spike interval of less than 8 ms occurring within 10 ms of defined canonical burst times. The burst time was defined as the first spike in that burst for each rendition. A burst was included for further analysis if it was present in more than 90% of the trials. For each trial, a burst time was excluded if it was 2 standard deviations above the value predicted by the relationship between the mean burst times and the burst times from that trial. We established the speed of each syllable rendition unilaterally by measuring the slope of the deviation from the mean burst times of that hemisphere. To determine the precision of burst times for each hemisphere, we measured the residual between each burst time and the consensus best fit line calculated using all burst times that met our criteria for each trial from both hemispheres. To determine the precision of bilateral coordination for each burst time, we calculated the residual between that burst time and the best fit line for all other burst times in each hemisphere. For each trial, residuals were calculated separately for ipsilateral and contralateral fits, with the burst in question held out for determining the best fit line.

#### *Eye tracking*

Custom MATLAB code was used to extract the luminance values for all frames acquired with hand-drawn ROIs. Once each frame was categorized as open or closed using thresholds determined for each eye in each recording, a moving average was taken (100 second boxcar kernel, 10 second step size).

#### *Temperature and bursting*

All temperature traces were smoothed with a 100-second boxcar kernel using a 10 second step size. The percent time a given neuron spent bursting was calculated throughout the recording using a 100 second window (step size: 10 sec, bursting criteria: instantaneous firing > 100 Hz). Pairwise comparisons for both temperature and bursting were made by taking 5000-second snippets from one hemisphere and comparing (Pearson's correlation) to either the time-matched snippet or to a randomly chosen epoch from the other hemisphere. For the bursting values, each neuron received an average r-value consisting of the mean of time-matched comparisons for all ipsilateral pairs, all contralateral pairs and a null value consisting of an average of shuffled comparisons. To

combine these measures, we calculated the cross-correlation between the temperature trace and the average of single neuron bursting (see below) for all recorded neurons (Figure S2). Using the resulting lag, we shifted the temperature trace in time and recalculated the correlation.

### *Population bursting*

Population bursting throughout the recording was defined by the percent of the population that met our bursting criteria (instantaneous firing rate of each neuron: > 100 Hz) in 5 ms bins, smoothed with a 150 ms boxcar kernel. We determined appropriate bursting thresholds by assessing the split between the bimodal distributions of the percentage of the population bursting. Thresholds were manually optimized to detect population bursting events for song (range: 4.75 – 10.5%) and sleep (range: 2.5 – 4%) for each hemisphere of each bird. Burst synchrony was defined as the percent of total bursting in both hemispheres within variable time windows (range: 1 ms–100 sec). To determine if the synchrony measured with a 1 ms window was above that expected by chance, we created a shuffled distribution of burst synchrony by randomly concatenating the measured burst times and inter-burst-intervals for each hemisphere and quantifying the resulting overlap.

### *Template matching*

The template matching strategy used here was recently developed by our laboratory.[24] A single template was made from the bursting activity of the population of RA neurons during the performance of each recorded vocalization: an introductory note, a single song rendition, and a distance call. The activity of each neuron was binarized based on its instantaneous firing rate (rate: > 100Hz). The data were then binned (bin width: 6 ms, step size: 3 ms) and further binarized; if a neuron was bursting within that bin, it was assigned a value of 1; no bursting was assigned a 0. Binarized and binned activity throughout sleep was assigned to the template bin it most resembles (Pearson's correlation). Template matching was performed separately for each hemisphere.

Our previous work showed that sleep replay in the zebra finch brain occurs at about the same speed as the song itself,[24] which translates to diagonal stretches with a slope of ~1 in 2D space created by plotting time in recording against the assigned time in the template. We therefore isolated replay events by filtering the template matching results. First, we removed the low-density bin assignments (those with fewer than four neighbors within 20 ms) and those assignments that did not meet our population bursting criteria (see above). Next, we limited our analysis to the resulting high density 'islands' with slopes between 0.5 and 1.5. The events that met our criteria during the 'lights off' period were considered sleep replay, and the events detected during the 'lights on' period were used to assess the synchrony of the hemispheres during vocalizations. Finally, we measured the distance between the assigned template matching results in each hemisphere when both hemispheres were participating in song-related activity.

## Quantification and statistical analysis

All statistical details of experiments can be found in figure legends and the results section, including the statistical tests used, the exact value of n, and what n represents (e.g., number of animals, number of cells, etc.). Values are reported as mean ± SD unless mentioned otherwise. Normal distribution of data was not assumed. No data were excluded from analysis. Statistical calculations were performed using MATLAB R2021a.